J. Comp. App. Res. Mech. Eng. Vol. 13. No. 2, pp. 181-190, 2024 *DOI: 10.22061/JCARME.2023.9064.2223*

Journal of Computational and Applied Research in Mechanical Engineering
jcarme.sru.ac.ir
SRTTU
JCARME
ISSN: 2228-7922

Research paper

Evaluation of omega-shaped Coriolis mass flow meter for laminar flow

Vikram A. Kolhe[a,*], Suyash Y. Pawar[b], Vishal D. Chaudhari[c], Ravindra L. Edlabadkar[d] and Kailas V. Chandratre[e]

[a]*Late G.N. Spakal Gurudev College of Engineering, Department of Mechanical Engineering, Nashik, Maharashtra, India*
[b]*MVPS's KBT College of Engineering, Department of Mechanical Engineering, Nashik, Maharashtra, India*
[c]*Cusrow Wadia Institute of Technology, Department of Mechanical Engineering, Pune, Maharashtra, India*
[d]*PVG's College of Engineering and Technology, Department of Mechanical Engineering, Pune, Maharashtra, India*
[e]*Department of Mechanical Engineering, KVN NSPS's LGM Institute of Engineering Education and Research Nashik, Maharashtra, India*

Article info:

Article history:

Received: 25/05/2022
Accepted: 05/07/2023
Revised: 08/07/2023
Online: 11/07/2023

Keywords:

Coriolis mass flow meter,
Omega tube configuration,
Fluid-structure interaction,
Experimentation,
Laminar flow regime.

[*]**Corresponding author:**
kolhe.vikram@gmail.com

Abstract

Measuring flow rate precisely in laminar flow has been a difficult task, especially when utilizing a Coriolis mass flow meter (CMFM) for low flow rate measurements. The meter often under-reads the mass flow rate, making it less useful in these conditions. The dominant factor affecting the CMFM's performance in laminar regions is secondary flow, which overshadows the generated Coriolis force, leading to an under-reading of the flow rate. Previous studies have indicated that tube curvature is the most significant parameter affecting secondary flow generation and the overall performance of the meter. An omega-shaped tube configuration featuring a continuous curvature has been identified as the optimal shape for maximizing the performance of a CMFM device in laminar flow. The purpose of the investigation is to study and compare the efficiency of various Omega tube designs that have undergone slight geometric alterations. Four different configurations were evaluated for maximum time lag by vibrating at their respective natural frequencies and keeping the sensor position along the centerline of the tube configuration.

1. Introduction

The Coriolis force produced by a fluid flowing through a sensor tube with a defined frequency of vibration forms the basis of the Coriolis mass flow meter (CMFM) principle. The mass flow rate of the fluid traveling through the tube is determined by measuring the tube twist caused by the fluid flow. As the flow rate increases, the tube twist also increases, but the range of the tube twist is significantly shorter. In laminar

flow, the performance of the meter is further reduced due to the generation of secondary flow, which limits its usefulness for flow measurement in this region. Kumar and Anklin [1] pointed out the influence of secondary flow on the functionality of a commercial meter consisting of twin U-shaped sensor tubes in low Reynolds number (Re) flow. A secondary shear force was noted to be responsible for diminishing the effect of the generated Coriolis force, thus highlighting a thrust for additional investigation to the configuration and proportions of the tube at low Re. A noticeable loss in meter sensitivity has been observed by Bobovnik *et al.* [2] while analyzing the influence of velocity profile on meter performance in the low-Re region. A straight tube with different aspect ratios has been considered for investigation. Using CFD numerical simulations, Kutin *et al.* [3] discussed the implications of the velocity profile for a straight tube meter vibrating in the beam and shell modes and noted that at low Reynolds numbers, intense changes in the velocity profile lead to intense deviations in meter sensitivity.

Few researchers have made attempts to compare the performances of sensor tubes with different configurations to identify the parameters yielding the maximum deformation of the sensor tube. The analysis of a U-shaped sensor tube with various L/D ratios (ratio of length of the tube to distance between two limbs of the U tube) and excitation frequencies for the lowest error was presented by Patil *et al.* [4]. To determine the ideal levels of variables, such as sensor position and vibration frequency, for maximum tube twist in a copper Omega (triangular)-shaped tube configuration, Patil *et al.* [5] used the design of experiments and response surface modeling methods. Patil *et al.* [6] modeled the tube twist and mass flow rate using the ANFIS (Adaptive Neuro Fuzzy Inference System) to predict the effects of various design parameters and tube material [7] on the performance of copper Omega (triangular tube shape)-type CMFM. The input-output relationship can be accurately predicted using the experimental data that is currently accessible using ANFIS, according to the authors. The flow rate of an Omega (triangular tube shape)-type CMFM was also estimated using a neural network method by Patil *et al.* [8, 9], who also found good agreement between the predicted and experimental results.

Bobovnik *et al.* [10] analyzed numerically the installation effects for a single straight tube, considering three flow disturbance elements such as a single elbow, a double elbow out of the plane, and an orifice in the steady-state condition of the tube. The disturbed flow due to the above elements has been recorded in terms of a change in flowmeter sensitivity. The study pointed out that the distribution of the fluid forces acting on the walls of the measurement tube when it is situated in a disturbed flow differs from the one in fully formed flow conditions. This is interpreted as a shift in the Coriolis meter's relative sensitivity. Kutin *et al.* [11] presented the effect of velocity profile on a derived asymptotic model for straight pipe clamped at both ends with fluid dynamic loading. To express the effect of the velocity profile, the effects of three components—translational, Coriolis, and centrifugal acceleration—and related correction factors have been taken into consideration.

The effects of braces and tube length for a U-shaped tube with and without sensor mass and driver mass on the time shift for two distinct turbulence models were studied by Shavrina *et al.* [12]. During validation, a discrepancy of less than 5% between simulation results and earlier experimental data was observed. Using the COMSOL simulation software, Hu *et al.* [13] performed a fluid-structure interaction study on a dual U-shaped meter and created a platform for meter design. The study discussed the impact of structural imbalance and the calculation of fluid viscosity based on the pressure difference between the meter's inlet and exit. Baker [14, 15], Wang, and Baker [16] presented a detailed review of CMFM based on published research and the industrial design of the meters. They have mentioned the technological development and further scope for improvement of the meter performance. For various tube configurations in the laminar flow regime, Kolhe *et al.* [17] conducted a thorough analysis of the effects of several factors, including tube configuration, excitation frequency, magnitude of excitation, and sensor position. Although it has been found that the Omega tube configuration has the

highest time lag readings in the laminar regime, there is still a dearth of scientific information regarding this configuration in the literature.
The purpose of the present work is to evaluate the performance of four alternative Omega tube configurations with slight geometrical differences. This study is unique in that it compares various Omega tube configurations to identify the one that results in the greatest phase shift in the laminar flow region through simulation and testing.

2. Omega tube configurations

2.1. Design of omega tube configuration

An accurate and stable mass flow rate in CMFM is primarily related to an adequate signal-to-noise ratio (i.e. desired outcome - time lag to undesired value) and sufficient strength of the Coriolis force [16]. Both of these factors are determined by the design parameters of the CMFM. The most important design factors for achieving significant tube deformation and accuracy in flow measurement are the tube geometry, vibration amplitude, drive frequency, and tube length. The amount of tube deformation brought on by the Coriolis force is also influenced by the elastic modulus of the tube, commonly referred to as the spring constant. With a given Coriolis force, a rise in the spring constant tends to lower deformation. Designing a CMFM should therefore emphasize selecting a reduced spring constant, which results in greater deformation, as well as producing the highest Coriolis force. For large sensitivity of the CMFM, the design objectives can be higher inlet and outlet arm lengths, or the greatest distance between the point of excitation and the axis of vibration, lower spring constant in terms of thin-wall tubing, and vibrating the tube at the natural or high excitation frequency [15, 16]. Pressure drop, tube thickness, and tube fatigue failure are the restrictions affecting the aforementioned design objectives.
The Omega tube configuration has been determined with the specified geometrical characteristics based on the tube configuration investigated by Kolhe *et al.* [17]. The first Omega tube configuration (model O1, Fig. 1(a)) has been designed with a 140 mm curvature radius, 50 mm inlet and outlet bend radii, and a 1 m long test section (i.e. length of the tube from the first inlet bend to the last exit bend). As mentioned earlier, achieving a higher tube length with sufficient curvature is one of the design goals. Therefore, the next Omega model, O2, has been created by increasing the curvature radius by 25%, as shown in Fig. 1(b). To target the second design goal, the model O1 has been redesigned with 100 mm inlet and outlet arm lengths (model O3, Fig. 1(c)). Furthermore, to maintain the test section length at 1 m, the curvature radius has been reduced to 110 mm (model O4, Fig. 1(d)). All the selected models of Omega tube shape have been designed with adequate hydrodynamic entrance length [18] to ensure a fully developed flow at the tube entry.

2.2. Modelling and simulation procedure

The selected Omega-shaped tube configurations were evaluated for a range of Re (600, 1200, and 1800) covering the laminar regime at the respective natural frequency of each configuration. Kolhe *et al.* [17] estimated the performance of the Omega-shaped tube (O1 model), as illustrated in Fig. 2, for three different sensor positions (SP1, SP2, and SP3) and frequencies (F1, F2, and F3, F2 being the natural frequency). They have reported that the sensor location SP2 (along the horizontal centerline of the tube configuration) and the natural frequency F2 of the tube excitation yield the maximum time lag results in the low Re regime. Therefore, the above-selected models of Omega tube configurations were evaluated with the sensor position at SP2 along with the respective natural frequencies of the tube configurations. Moreover, to study the influence of the elastic module (spring constant) of tube material, this analysis has been extended to two different tube materials, viz. Stainless steel (SS 304) and copper. The input parameters and properties of the selected tube materials have been listed in Table 1.

2.3. Natural frequencies of the tube configurations

Utilizing ANSYS 19.2, the natural frequencies of the specified Omega tube models have been calculated. The fundamental modes of the

selected Omega models of SS 304, along with their corresponding natural frequencies are depicted in Fig. 3. It can be noted that the shape and material of the CMFM tube influence the natural frequency of the tube section. The natural frequencies of the upper Omega models were found to be lower than those of the SS 304 models, as mentioned in Table 2.

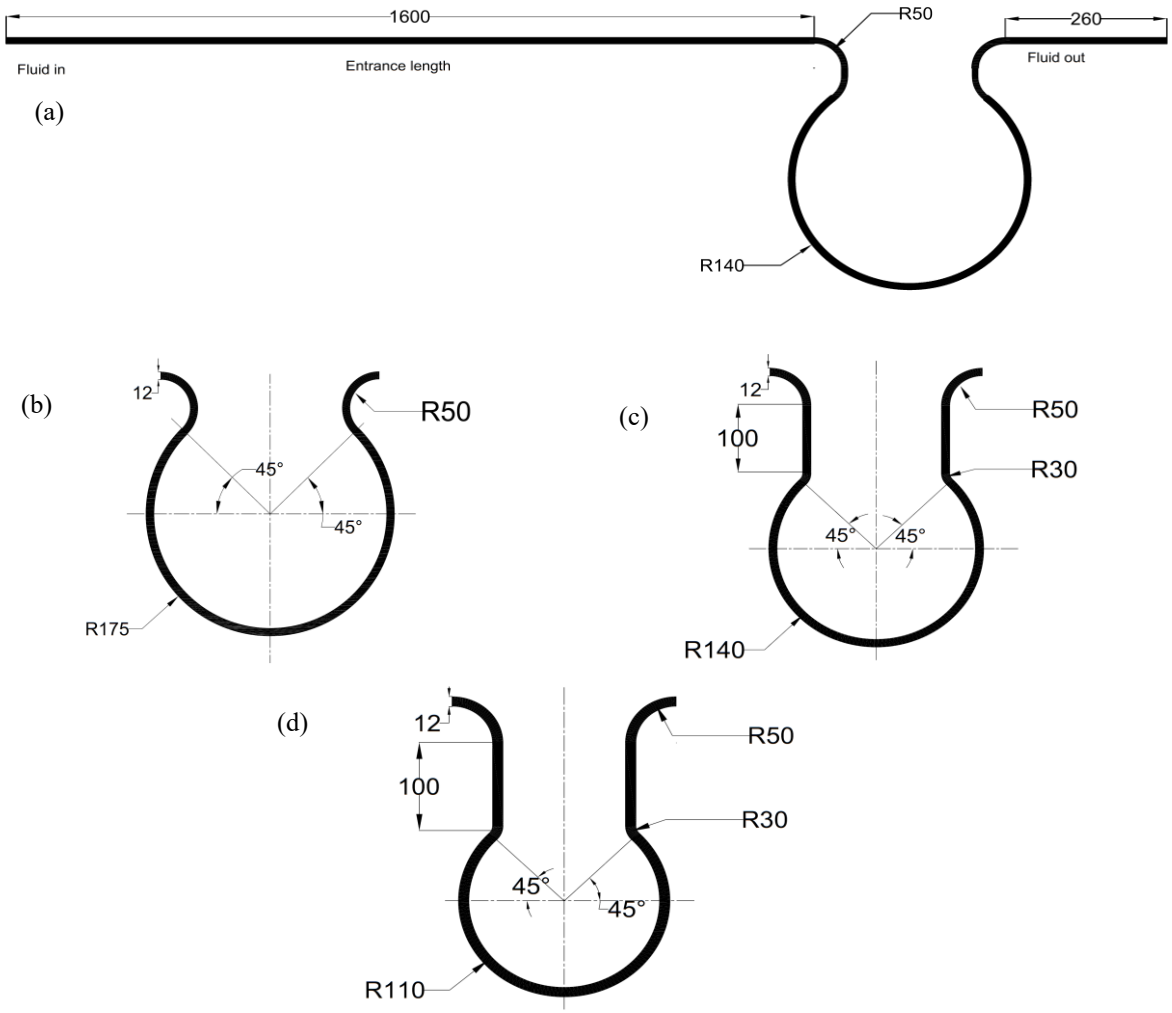

Fig. 1. Models of Omega shaped tube configuration; (a) O1, (b) O2, (c) O3, and (d) O4.

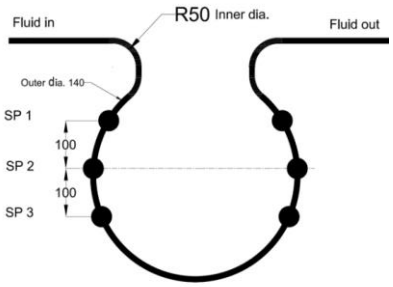

Fig. 2. Sensor positions for the Omega tube configuration (O1 model).

Table 1. Input parameters.

Parameter	Details
Tube material	SS 304 (Young's Modulus, E = 210 GPa, Density, ρ = 8000 kg/m^3, Poisson's ratio, ν = 0.29) Copper (Young's Modulus, E = 121 GPa, Density, ρ = 8960 kg/m^3, Poisson's ratio, ν = 0.34)
Tube dimensions	Internal diameter Di = 12 mm, Thickness = 1.3 mm
Sensor location	Along the horizontal centreline of tube configuration on inlet and outlet limbs
Drive frequency	Natural frequency
Flow range	Re = 600-1800
Amplitude of vibration	6 mm peak to peak
Fluid	Water (Density, ρ = 1000 kg/m^3, Dynamic viscosity, μ = 0.00089 Pa.s at 25 °C)

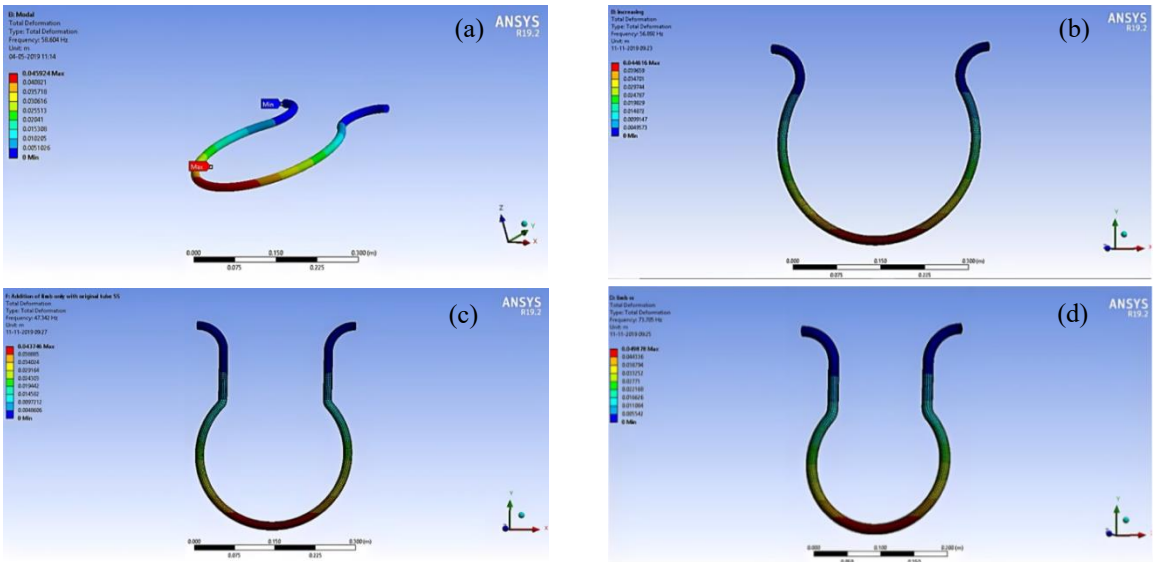

Fig. 3. Fundamental modes of vibration of selected Omega models of SS 304 (a) O1, (b) O2, (c) O3, and (d) O4.

Table 2. Natural frequencies of selected Omega models by modal analysis.

Tube model	Natural frequency (Hz)	
	SS 304	Copper
Model O1	58.6	56.87
Model O2	56.89	51.53
Model O3	47.3	43.22
Model O4	73.7	66.76

3. Fluid structure interaction (FSI)

Fluid-structure interaction can be used to investigate situations where fluid flow and structure movement are present. In the present work, ANSYS 19.2 has been implemented for building the fluid flow and tube motion to predict the results of time lag. The accuracy of numerical simulation and processing time are both known to be affected by meshing. The system-generated meshing is used for structure and fluid in the current simulation. The mesh adjacent to the wall should be fine enough to resolve the boundary layer flow. The program-controlled inflation in the boundary layer has been adapted for the meshing of fluid and structure. Two-way coupled FSI was performed for the selected Omega tube configurations to interpret the time lag results. In all cases, the tubes were excited using an external periodic force with an amplitude of excitation equal to 6 mm, as well as at the respective natural frequency of each configuration, as displayed in Fig. 4.

The computational time was controlled by adjusting the mesh quality. To determine the time lag readings, a mathematical tool was used to solve the directional deformations of the two arms of the tube. The fluid travelling through the sensor tube in the current study was presumed to be isothermal, Newtonian, and incompressible.

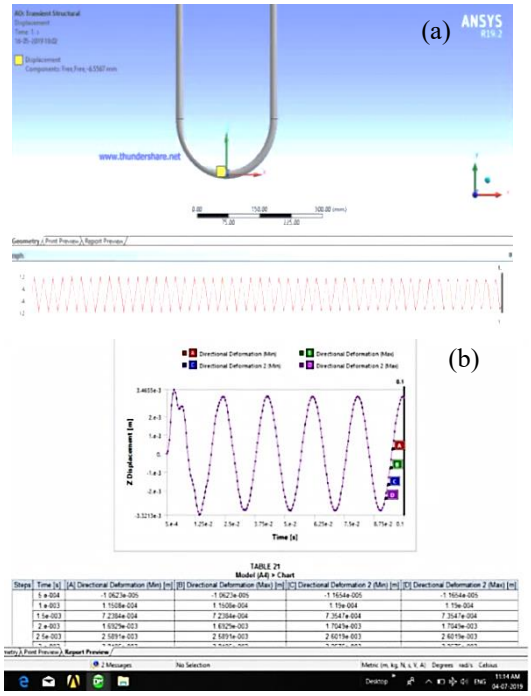

Fig. 4. FSI of Omega tube configuration; (a) Transient structural displacement of the tube and (b) Displacement of nodes of two limbs in Y direction.

The mesh movement (or boundary movement) must be taken into account for both the fluid and the structure while simulating the CMFM-linked approach. The fluid flowing through the vibrating tube adds to the motion, which further exerts a reactive force on the tube (structure) due to its inertia. The tube displacements that result from this force application indicate changes in the vibratory behavior of the structure. The experimentation using the same input conditions for the chosen tube designs served to confirm the findings of the FSI exercise.

4. Experimental analysis

4.1. Experimental set-up

An experimental facility was developed to accommodate the CMFM with selected Omega tube configurations. The setup facilitates the variation of investigation parameters over a range. The experiments were conducted at room temperature with water as the flowing fluid. The actual flow rate was determined using the conventional method of collecting the fluid in a calibrated container for a specific period of time. Water supply to the test tube configurations was provided through an overhead tank elevated approximately 10 m above the ground. Two ball valves were used to control the water flow rate to the test tube section. The ball valve at the inlet of the entrance length was always kept fully open to avoid any air bubbles in the flow, whereas the valve provided at the exit of the tube section was used to maintain the Reynolds number at a particular value.

An electromagnetic vibration exciter with a power oscillator was used to provide oscillatory motion to the tube configurations at the operating frequency, as shown in Fig. 5. The amplitude and vibration frequency were adjusted to the required values using a power amplifier. Since the exciter produced strong and frequent vibrations, it was mounted on a heavy foundation to damp the vibrations and prevent them from transferring to other components like sensors and the time lag measurement unit. A plywood structure was constructed to support the tube configuration with hydrodynamic length. It was completely isolated from the exciter, while the sensor tubes were clamped to the plywood structure at their ends using rubber pads to damp the external vibrations. The deflection of the tube section on the inlet and outlet sides of the flow was sensed by using two infrared sensors, as shown in Fig. 5.

The Coriolis force generated due to the interaction between excitation and the change in momentum of the flowing fluid causes a phase shift between the limbs of the meter tube, which is proportional to the mass flow rate of the flowing fluid. The phase shift is detected by the displacement sensors in terms of a time lag in microseconds. The location of the sensors affects the measurement of the phase shift. It has already been reported that the sensor position, SP2 (i.e., along the centerline of the circular section), was the optimum position for maximum time lag results [17]. Hence, in all cases, the sensor position was maintained at SP2 and the tubes were excited at their natural frequencies.

4.2. Experimental procedure

The fidelity of the sensors was guaranteed in a no-flow situation by ensuring a zero reading at the start of each reading cycle. The water temperature was measured using a thermometer, and the flow rate was controlled by adjusting the

opening of the outlet ball valve to set the flow at a predetermined rate. The discharge was measured at the beginning and end of the reading cycle to ensure measurement accuracy. The sensor location was adjusted to be along the centerline of the tube configuration as selected in the numerical simulation. The vibration exciter was set to the natural frequency as selected in the numerical simulation, and the amplitude of the tube vibration was maintained at 6 mm peak to peak throughout the experimentation. The time lag (Δt) readings were recorded using the time lag measurement unit for a time period of 120s and then averaged. This process was repeated for a range of Reynolds numbers in the laminar flow regime, and the time lag (Δt) readings for certain flows were repeated to eliminate errors in measurements.

5. Results and discussion

For the SS 304 and copper Omega models, the results have been plotted as time lag vs. Reynolds number (Re), as seen in Figs. 6 and 7, respectively. The experimental and numerical results of time lag values were compared for the selected tube configurations. The comparison was conducted using the identical drive frequency, excitation amplitude, and sensor position parameters that were taken into account in the FSI analysis. However, it was challenging to achieve the precise values of Re during experimentation used in FSI. Therefore, in experimentation, the Re values nearer to the values chosen for the FSI are maintained.

It may be concluded that the FSI results and the experimental findings are in good agreement. Both analyses have shown a sluggish response to changes in mass flow in the laminar region. However, after a Re equal to 1300 to 1400, a noticeable response has been shown by almost all the models of the Omega tube configuration. When compared to its predecessors for both materials, the original Omega tube O1 model had the largest time lag values at natural frequency. Furthermore, it demonstrated a notable and linear performance, establishing its eligibility for flow measurement in the laminar flow region.

Fig. 5. Experimental set-up for the Omega models.

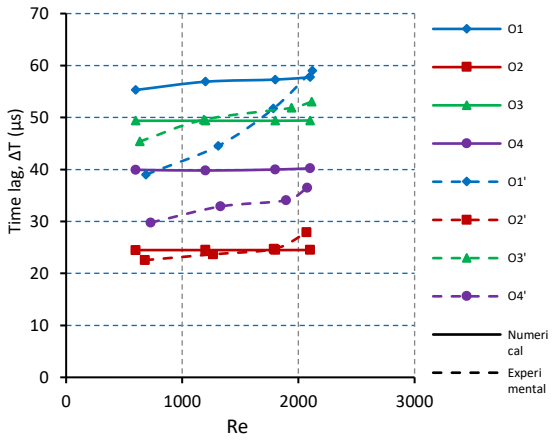

Fig. 6. Time lag vs. Re at natural frequency for the four Omega models of SS 304.

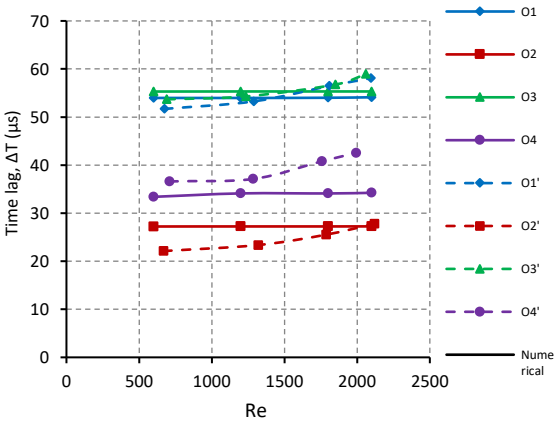

Fig. 7. Time lag vs. Re at natural frequency for the four Omega models of copper.

The O2 model (SS 304) having an increased curvature diameter, which indirectly increased the distance between the inlet and outlet bends, showed modest sensitivity to flow rate variations for both SS 304 and copper materials. The third model, O3, of the Omega tube configuration with the addition of limbs to the O1 model, recorded the second largest range of time lag readings; however, it manifested a quite sluggish response. The O4 model, which has limbs with a decreased diameter in comparison to the O1, was also found to have low sensitivity to flow variations. However, the O4 model was found to be more responsive as compared to the O2 model.

Overall, it has been found that the original O1 model of SS 304 is more responsive than its competitors, with the O3 model getting in at second place but with a slow reaction, the O4 model coming in at third place, and the model O2 being discovered to be unresponsive and occupying the bottom position. The O1 and O3 models of copper (the original Omega and the addition of limbs) were found to have comparable time lag reading ranges, although O1 was discovered to be more responsive to flow variations than O3.

The O4 model ranked third, taking into account its response to changes in flow rate, while the O2 model recorded the lowest range of time lag readings with the lowest sensitivity when compared to its competitors for both materials.

The overview of numerical and experimental values for time lag measurements is shown in Tables 3 and 4.

Table 3. Summary of numerical (FSI) and experimental results of time lag for selected models of Omega-shaped tube of SS 304 ($600 \leq Re \leq 2200$).

Tube model	Time lag range, Δt (μs)	
	FSI simulation results	Experimental results
O1	$55.2973 \leq \Delta t \leq 57.749$	$39.02 \leq \Delta t \leq 59.0178$
O2	$24.4883 \leq \Delta t \leq 24.5055$	$22.557 \leq \Delta t \leq 27.8813$
O3	$49.375 \leq \Delta t \leq 49.43$	$45.3832 \leq \Delta t \leq 53.0492$
O4	$33.401 \leq \Delta t \leq 24.239$	$29.7829 \leq \Delta t \leq 36.475$

Table 4. Summary of numerical (FSI) and experimental results of time lag for selected models of Omega-shaped tube of copper ($600 \leq Re \leq 2200$).

Tube model	Time lag range, Δt (μs)	
	FSI simulation results	Experimental results
O1	$53.98 \leq \Delta t \leq 54.119$	$41.693 \leq \Delta t \leq 56.0897$
O2	$27.2269 \leq \Delta t \leq 27.2511$	$22.1151 \leq \Delta t \leq 27.7868$
O3	$55.307 \leq \Delta t \leq 55.329$	$43.6873 \leq \Delta t \leq 48.9384$
O4	$39.929 \leq \Delta t \leq 40.221$	$611 \leq \Delta t \leq 32.5298$

5. Conclusions

From the analysis of the results of this investigation, the following conclusions may be drawn:

- The material and shape of the tube section of CMFM have a big impact on the natural frequency of the tube segment.
- The natural frequencies of the copper Omega models have been found to be lower than those of the SS 304 versions.
- The Omega tube's original O1 model

recorded the highest time lag measurements at its natural frequency when compared to other models for both materials. Additionally, it showed apparent and linear performance, making it an acceptable choice for flow measurement in the laminar flow region.

- An increase in curvature diameter—which, in the O2 model, indirectly leads to an increase in the distance between the inlet and outlet bends—showed little sensitivity to changes in flow rate for both SS 304 and copper materials.
- The second-largest range of time lag values was produced by adding limbs to the original O1 model of SS 304 (model O3), although it showed a slower response time than the O1 model. Additionally, the O4 model's insertion of limbs with smaller diameters demonstrated little sensitivity to variations in flow rate.
- The O2 model, on the other hand, showed a narrow range of time lag readings and lacked sensitivity in comparison to the other models for both materials, while the O4 model was discovered to be more sensitive.
- It can be inferred that the O1 type of Omega tube configuration of both SS 304 and copper is the best tube configuration, showing optimum performance for measuring flow rates in the laminar regime.

References

[1] V. Kumar and M. Anklin, "Numerical Simulations of Coriolis Flow Meters for Low Reynolds Number Flows," *J. Metrol. Soc. India*, Vol. 26, No. 3, pp. 225–235, (2011).

[2] G. Bobovnik, J. Kutin and I. Bajsic, "Estimation of Velocity Profile Effects in the Shell-type Coriolis Flowmeter using CFD Simulations," *Flow Meas. Instrum.*, Vol. 16, No. 6, pp. 365–373, (2005).

[3] J. Kutin, G. Bobovnik, J. Hemp and I. Bajsic, "Velocity Profile Effects in Coriolis Mass Flowmeters: Recent findings and open questions," *Flow Meas. Instrum.*, Vol. 17, No. 6, pp. 349–358, (2006).

[4] S. Sharma, P. Patil, M. Vasudev and S. Jain, "Performance Evaluation of an Indigenously Designed Copper (U) Tube Coriolis Mass Flow Sensors," *J. Meas.*, Vol. 43, No. 9, pp. 1165–1172, (2010).

[5] P. Patil, S. Sharma and S. Jain, "Response Surface Modeling of Vibrating Omega Tube (Copper) Electromechanical Coriolis Mass Flow Sensor," *Expert Syst. Appl.*, Vol. 39, No. 4, pp. 4418–4426, (2012).

[6] P. Patil, S. Sharma and S. Jain, "Performance Evaluation of a Copper Omega Type Coriolis Mass Flow Sensor with an Aid of ANFIS Tool," *Expert Syst. Appl.*, Vol. 39, No. 5, pp. 5019–5024, (2012).

[7] P. Patil, S. Sharma, H. Jaiswal and A. Kumar, "Modeling Influence of Tube Material on Vibration Based EMMFs Using ANFIS," *Procedia Mater. Sci., 3rd Int. Conf. "Materials Processing and Characterisation",* Vol. 6, pp. 1097-1103, (2014).

[8] P. Patil, S. Sharma and S. Jain, "Prediction Modeling of Coriolis Type Mass Flow Sensor using Neural Network," *Instrum. Exp. Tech.*, Vol. 54, No. 3, pp. 435–439. 2011.

[9] P. Patil, S. Sharma, V. Paliwal and A. Kumar, "ANN Modelling of Cu Type Omega Vibration Based Mass Flow Sensor", *Procedia Technol., 2nd Int. Conf. "Innovations in Automation and Mechatronics Engineering",* Vol. 14, pp. 260–265, (2014).

[10] G. Bobovnik, J. Kutin, N. Mole, B. Stok and I. Bajsic, "Numerical Analysis of Installation Effects in Coriolis Flowmeters : A Case Study of a Short Straight Tube Full-Bore Design," *Flow Meas. Instrum.* Vol. 34, pp. 142–150, (2013).

[11] J. Kutin and I. Bajsic, "Fluid-Dynamic Loading of Pipes Conveying Fluid with a Laminar Mean-Flow Velocity Profile," *J. Fluids Struct.,* Vol. 50, pp. 171–183, (2014).

[12] E. Shavrina, V. Nguyen, Z. Yan and B. Khoo, "Fluid-Solid Interaction

Simulation Methodology for Coriolis Flowmeter Operation Analysis", *Sensors*, Vol. 21, No. 23, 1-20, (2021).

[13] Y. Hu, Z. Chen and P. Chang, "Fluid–Structure Coupling Effects in a Dual U-Tube Coriolis Mass Flow Meter", *Sensors*, Vol. 21 , No. 3, 1-30, (2021).

[14] R. Baker, "Coriolis Flowmeters: Industrial Practice and Published Information," *Flow Meas. Instrum.*, Vol. 5, No. 4, pp. 229-246, (1994).

[15] R. Baker, *Flow Measurement Handbook*, Cambridge University Press, New York, pp. 398-426, (2000).

[16] T. Wang and R. Baker, "Coriolis Flowmeters: a Review of Developments over the Past 20 Years, and an Assessment of the State of the Art and Likely Future Directions," *Flow Meas. Inrtrum.*, Vol. 40, pp. 99-123, (2014).

[17] V. Kolhe and R. Edlabadkar, "Performance Evaluation of Coriolis Mass Flow Meter in Laminar Flow Regime", *Flow Meas. Instrum.*, Vol. 77, pp. 1-13, (2021).

[18] F. M. White, *Fluid Mechanics*, 7th ed., McGraw-Hill, New York, pp. 347-355, (2011).

How to cite this paper:

Vikram A. Kolhe, Suyash Y. Pawar, Vishal D. Chaudhari, Ravindra L. Edlabadkar and Kailas V. Chandratre, " Evaluation of omega-shaped Coriolis mass flow meter for laminar flow,", *J. Comput. Appl. Res. Mech. Eng.*, Vol. 13, No. 2, pp. 181-190, (2024).

DOI: 1010.22061/JCARME.2023.9064.2223

URL: https://jcarme.sru.ac.ir/?_action=showPDF&article=1904